Direct Observation of Terahertz Surface Modes in Nanometer-Sized Liquid Water Pools

Joel E. Boyd, Ari Briskman, and Vicki L. Colvin,
Department of Chemistry, Rice University, MS-60, P.O. Box 1892, Houston, Texas 77251

Daniel M. Mittleman*
Department of Electrical and Computer Engineering, Rice University, MS-366, P.O. Box 1892, Houston, Texas 77251
(Received 16 April 2001; published 18 September 2001)

The far-infrared absorption spectrum of nanometer-sized water pools at the core of AOT micelles exhibits a pronounced resonance which is absent in bulk water. The amplitude and spectral position of this resonance are sensitive to the size of the confined water core. This resonance results from size-dependent modifications in the vibrational density of states, and thus has far-reaching implications for chemical processes which involve water sequestered within small cavities. These data represent the first study of the terahertz dielectric properties of confined liquids.

DOI: 10.1103/PhysRevLett.87.147401 PACS numbers: 78.30.Cp, 77.22.–d, 78.66.Vs

The low-frequency vibrational modes of water confined on the nanometer scale are significant in many different fields. Layers of both strongly and weakly associated water molecules surround most biomolecules, and play a critical role in structural [1–3] and dynamical [4,5] processes. When the water is confined in three dimensions, these effects may be even more dramatic. For example, the low-frequency modes of water clusters are involved in the allosteric regulation of hemoglobin [6] and in the relaxation dynamics of a variety of proteins [7,8]. The structuring of liquids on these length scales is thought to be important in the liquid-to-glass transition [9,10]. A modification of the vibrational mode structure induced by nanometer-scale confinement has also been suggested by molecular dynamics simulations [11,12], and observed in microemulsion systems using neutron and light scattering techniques [13,14]. Another experimental probe of these vibrational modes is dielectric spectroscopy. Not only can this provide information about the vibrational density of states, but it also measures a parameter of fundamental importance in many liquid phase reactions. Although the dielectric properties of confined liquids have been studied at GHz frequencies [15,16], the terahertz spectral range, where the collective modes of liquids are most evident, has not been explored.

In this Letter we report measurements of the far-infrared dielectric of a model system for confined water, inverse micelles. The spectrum of the liquid at the micelle core exhibits a pronounced absorption resonance in the THz range ($3-33\ \mathrm{cm}^{-1}$), the properties of which depend sensitively on the size of the water pool. This can be understood in terms of the mode spectrum of a small spherical droplet [17], in which a significant fraction of the vibrational degrees of freedom are manifested as surface-localized modes. These surface modes or shape oscillations have been predicted for a variety of micellar systems [18], and play an increasingly important role in the vibrational density of states as the micelle size decreases. Since the restructuring of the mode spectrum described here is a direct consequence of the geometrical confinement, these results illustrate the importance of cavity size in determining the properties of nanoscale water. In particular, their infrared activity leads to a complicated size-dependent dielectric function.

Our experiments involve the measurement of the far-infrared dielectric properties of water confined in the core of inverse micelles. These systems, nanometer-sized water droplets stabilized in heptane by the surfactant sodium bis(2-ethylhexyl) sulfosuccinate (AOT), have been characterized extensively with respect to their size, shape, size dispersion [19,20], and the nature of the water pool at the core of the micelle [21,22]. For these measurements, AOT inverse micelles were prepared according to standard methods, using a surfactant purified as in Ref. [23]. By controlling the concentration ratio $w = [\mathrm{H_2O}]/[\mathrm{AOT}]$, one can vary the radius of the free water pool at the center of the micelle from $\sim$1 to 9 nm. Karl Fischer titration was used to verify that the native water content of the purified AOT is less than 1% by weight, leading to a negligible uncertainty in the average micelle size.

Far-infrared spectroscopy provides a direct probe of the picosecond dynamics of liquids and is particularly sensitive to their collective vibrational modes [24,25]. We use terahertz time-domain spectroscopy [24–26], a technique which permits the generation and coherent detection of broadband electromagnetic transients in the far infrared. We employ a variable path cell with polyethylene windows to measure a series of transmitted THz waveforms at several different path lengths. Fourier analysis of these time-domain waveforms gives both the power absorption coefficient $\alpha(\nu)$ and the refractive index $n(\nu)$, and therefore the complex dielectric function $\varepsilon_{\mathrm{solution}}(\nu)$ [24].

To determine the complex dielectric of the water pool in the micelle interior, we perform a deconvolution of the raw data using an electrostatic core-shell dielectric model which contains no adjustable parameters. This model has been used extensively for many years to describe the high-frequency dielectric behavior of dilute dispersions of

concentric core-shell materials [27]. The dielectric of the micelle is related to that of the solution by

$$\frac{\varepsilon_{\text{solution}} - \varepsilon_{\text{micelle}}}{\varepsilon_{\text{background}} - \varepsilon_{\text{micelle}}} \left(\frac{\varepsilon_{\text{background}}}{\varepsilon_{\text{solution}}} \right)^{1/3} = 1 - \phi , \quad (1)$$

where ϕ is the volume fraction of micelles in solution and $\varepsilon_{\text{background}}$ is the dielectric of the nonaqueous phase, heptane. Once $\varepsilon_{\text{micelle}}$ is known, the dielectric of the aqueous core can be determined. To do so, one models the micelles as a spherical core $\varepsilon_{\text{core}}$ surrounded by a concentric shell. $\varepsilon_{\text{shell}}$ is determined by measuring the dielectric function of a reference solution, identical to the sample except that no water has been added ($w = 0$). It has been established that, in the absence of water, "dry" micelles form that are spherical and monodisperse, so the effective dielectric of the shell can be directly determined [21]. With knowledge of $\varepsilon_{\text{shell}}$, one may deconvolve the dielectric of the aqueous core, using

$$\varepsilon_{\text{core}} = \varepsilon_{\text{shell}} \left(\frac{2(1 - F)\varepsilon_{\text{shell}} - (2 + F)\varepsilon_{\text{micelle}}}{(1 + F)\varepsilon_{\text{micelle}} - (1 + 2F)\varepsilon_{\text{shell}}} \right), \quad (2)$$

where F is the volume fraction of the core within each micelle [28].

The applicability of this core-shell model to micellar systems is subject to several assumptions which are reasonable given prior studies on the structure of micelles. It relies on the assumption that the dielectric of the shell does not change appreciably when water is added to the core of the micelle. This seems reasonable, since the structural conformations of the surfactant molecules are essentially unchanged, and thus insensitive to water content over the entire size range studied [29]. The model ignores the size dispersion of the water pools, which has been estimated to be about 10% for AOT micelles [30]. It also neglects inhomogeneities within the aqueous core, which could arise from the structural rearrangement of the water or from the distribution of Na^+ cations, for example. The most striking approximation is that of an abrupt interface between the surfactant shell and the water core. Recent molecular dynamics simulations have indicated that this interface is only a few angstroms in width, so this is not an unreasonable description of AOT inverse micelles [31].

An important validation of our analysis method can be found in the inset of Fig. 1, which depicts the dielectric spectra of several samples using a Cole-Cole plot. This shows that the measured spectra for larger micelles approaches that of the bulk liquid [24]. The recovery of bulk dielectric properties in the largest micelles is consistent with the common description of a free water pool at the core of the micelles. However, as the micelle size is reduced, the absorption spectrum develops a pronounced resonance that grows and shifts to higher frequency with decreasing water pool radius. For the smallest micelles measured ($w = 10$), we observe a peak absorption $\sim$8 times larger than that of bulk water [24]. The circular

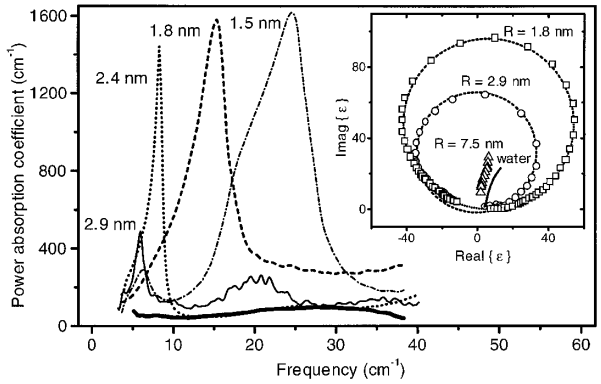

FIG. 1. Measured power absorption coefficients as a function of frequency for several representative micelle samples, as derived from $\varepsilon_{\text{core}}$ [see Eq. (2)]. The thick solid line shows a typical result for large micelles, with water pool radius $R = 75$ Å. The remaining curves are for micelle samples with water pool radii as labeled. The inset shows parametric Cole-Cole plots for several of these data sets. For the smaller micelles, the circular curves indicate that these modes are resonant and not overdamped. For the largest micelles (triangles), the result is quite similar to bulk water (solid line).

Cole-Cole plots emphasize the resonant nature of the absorption peaks shown in Fig. 1.

The approximate $1/R$ dependence of the absorption peak frequency suggests that confined acoustic vibrations play an important role. In order to understand the size dependence of the spectral location and amplitude of the observed absorptions, we adapted a description developed by Tamura and Ichinokawa for the vibrational mode spectrum of a small liquid droplet [17]. The modes are enumerated according to the well-known Debye criterion, in which a maximum eigenfrequency is determined by the total number of degrees of freedom. An additional criterion is imposed on the angular momentum quantum number L, to account for the atomicity of a real liquid. Essentially, the wavelength of the mode must be larger than the mean intermolecular distance. The eigenmodes divide into two distinct categories, one which represents surface vibrations (shape oscillations) and another which involves internal vibrations (compressional oscillations). These latter modes fall at frequencies larger than $\pi v_c/R$, where v_c is the speed of sound in the liquid and R is the radius of the spherical droplet. Using the bulk value for the sound velocity, one finds that the majority of these internal modes lie at frequencies above 1 THz, too high to explain the resonances observed in Fig. 1.

In contrast, the surface modes are lower-frequency excitations, lying closer to the range of the observed modes. These surface modes are harmonic shape oscillations arising from the restoring force associated with the interfacial tension at the micelle surface. The presence of the surfactant monolayer at the interface acts to substantially reduce this interfacial tension relative to that of a bare water-alkane interface, and thus shift these modes to lower frequencies. The mode frequencies are given by

$$\omega_L = \sqrt{\frac{\sigma(R)\,(L-1)\,(L+2)}{R^3[(\rho_{\text{water}}/L) + (\rho_{\text{heptane}}/(L+1))]}}, \quad (3)$$

where $\sigma(R)$ is the interfacial tension and ρ_{water} and ρ_{heptane} are the bulk liquid densities [17,18]. The size-dependent interfacial tension of an AOT micelle was considered in great detail by Peck and co-workers [32]. They developed an expression for $\sigma(R)$ which contains contributions from both the water-surfactant and the surfactant-oil interfaces. To extract a numerical value for $\sigma(R)$, one requires knowledge of several parameters, including the structural parameters for the AOT molecule, the counterion dissociation constant, the effective headgroup and tailgroup areas, and the solubility parameter for heptane [32]. We used literature values for all of these parameters [32]. This model predicts a monotonically decreasing $\sigma(R)$ with increasing radius due to the curvature-dependent electrostatic interaction of the headgroups.

By using this formalism to determine the interfacial tension, one can calculate the vibrational density of modes $D(\nu)$ [17]. This calculation contains no freely adjustable parameters. Results are presented in Fig. 2 for three different water pool radii. In each case, the contribution of the low-frequency shape oscillations is evident below 0.4 THz. As the radius decreases, this portion of the spectrum contains an increasing fraction of the total mode density, as anticipated. From these spectra, we may calculate the mean frequency of the surface modes, according to $\langle \nu_{\text{surface}} \rangle = \int_0^{\nu_S} \nu D(\nu)\, d\nu / \int_0^{\nu_S} D(\nu)\, d\nu$, where ν_S is the maximum surface mode frequency (Fig. 2, arrows). The size dependence of $\langle \nu_{\text{surface}} \rangle$ is shown in Fig. 3 (solid line). This result is an *a priori* prediction of the mean frequency, which can be compared to the experimental data. One can also extract from these calculations an estimation of the absorption strength. With the assumption that the total oscillator strength of the vibrational transitions is conserved, we estimate the absorption strength of the transition as the integrated surface mode density, normalized to the total number of modes. A comparison of this result with the experimental integrated absorption strength is shown in Fig. 4. Here, since the data are in arbitrary units, the calculation is scaled to match the experimental data point corresponding to the largest radius studied.

This simple model accurately predicts both the frequency of the induced absorption feature and the trend in its magnitude, for water pools larger than 2.5 nm radius. This agreement provides strong evidence that the observed perturbations to the dielectric function result from surface vibrations, whose number and spectral positions depend on the water pool size. However, for smaller micelles, it is clear that the model fails to capture both the strong blueshift of the peak frequency and the dramatic increase in absorption strength. This could be because of changes in the nature of the water pool as its size decreases. In the smallest micelles, a substantial fraction of the internal water is bound rather than free water [22]. The calculated surface tension relies on parameters, such as the interior liquid density and its static dielectric constant, which could be affected by the increasingly strained hydrogen bond network. The compressibility of the sequestered water is known to be larger than that of the bulk, but decreases with decreasing micelle size [33]. This decreasing compressibility corresponds to an additional stiffening

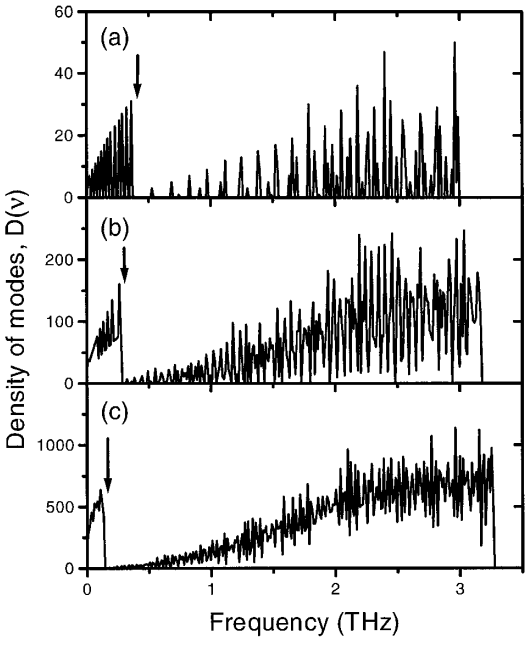

FIG. 2. Calculated vibrational density of modes of a spherical water droplet $D(\nu)$, for three different droplet radii: (a) $R = 2$ nm, (b) $R = 5$ nm, (c) $R = 9$ nm. These histograms have been calculated with a bin size of 12 GHz. The peak at the low-frequency end of the spectrum results from the surface vibrational modes (shape oscillations). The vertical arrows represent ν_S, the high-frequency cutoff of the surface mode contribution.

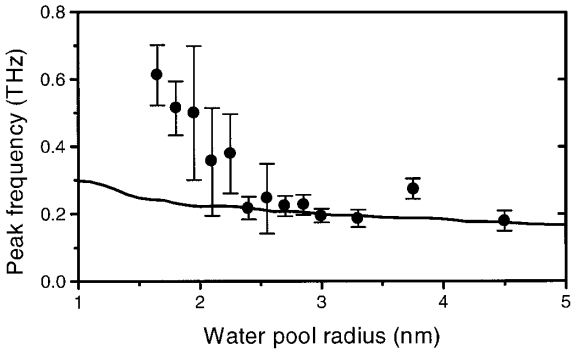

FIG. 3. Spectral position of the absorption resonance as a function of water pool radius. The solid curve shows the calculated mean surface mode frequency $\langle \nu_{\text{surface}} \rangle$. This *a priori* prediction of the size dependence of the peak frequency contains no adjustable parameters. The error bars indicate the standard deviation associated with repeated measurements.

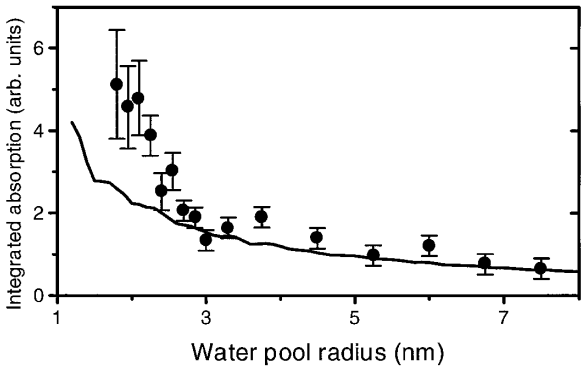

FIG. 4. Integrated absorption strength of the measured spectra as a function of water pool radius. The solid line shows the fraction of the total mode density contained in the surface modes. This *a priori* prediction of the size dependence of the absorption strength has been scaled to coincide with the data point for the largest micelle, $R = 7.5$ nm. Otherwise, there are no adjustable parameters in this calculation. The error bars indicate the standard deviation associated with repeated measurements.

of the micelle structure, which could lead to increased vibrational frequencies. Finally, our calculations have not accounted for selected rules on the vibrational transitions, which could have an influence on both the shape and amplitude of the measured peaks [34].

In conclusion, we report the first observation of surface vibrational modes in nanometer-sized liquid water pools. These are manifested as strong resonances in the terahertz absorption spectrum of the confined liquid. It should be noted that narrow well-resolved resonances are almost unprecedented in far-infrared liquid-state spectroscopy. These observations have important implications for any chemical, biological, or catalytic processes in which sequestered water plays a role. Since solvent vibrations are crucial in determining the rates of many chemical reactions, these results raise the intriguing possibility that the design of certain active biomolecular subunits may be optimized to exploit the enhanced vibrational density of states induced by the confinement.

This work was partially supported by the National Science Foundation (CHE-967020), and R. A. Welch foundation (C-1342), and the American Chemical Society Petroleum Research Fund (36088-G7). We gratefully acknowledge the assistance of Jared Turner of Dianal America for the Karl Fischer analysis.

*Email address: daniel@rice.edu

[1] J. L. Green, J. Fan, and C. A. Angell, J. Phys. Chem. **98**, 13 780 (1994).
[2] W. E. Royer *et al.,* Proc. Natl. Acad. Sci. U.S.A. **93**, 14 526 (1996).
[3] M.-C. Bellissent-Funel, J. Mol. Liq. **78**, 19 (1998).
[4] M. H. Vos *et al.,* Nature (London) **363**, 320 (1993).
[5] A. Paciaroni, A. R. Bizzarri, and S. Cannistraro, Phys. Rev. E **60**, 2476 (1999).
[6] M. F. Colombo, D. C. Rau, and V. A. Parsegian, Science **256**, 655 (1992).
[7] W. Doster *et al.,* Biophys. J. **50**, 213 (1986).
[8] V. P. Denisov and B. Halle, Faraday Discuss. Chem. Soc. **103**, 227 (1996).
[9] B. Frick and D. Richter, Science **267**, 1939 (1995).
[10] F. Sette *et al.,* Science **280**, 1550 (1998).
[11] J. Horbach *et al.,* Phys. Rev. E **54**, 5897 (1996).
[12] A. Paciaroni, A. R. Bizzarri, and S. Cannistraro, Phys. Rev. E **57**, 6277 (1998).
[13] B. Farago *et al.,* Phys. Rev. Lett. **65**, 3348 (1990).
[14] V. Lisy and B. Brutovsky, Phys. Rev. E **61**, 4045 (2000).
[15] Y. B. Mel'nichenko *et al.,* J. Chem. Phys. **103**, 2016 (1995).
[16] M. D'Angelo *et al.,* Phys. Rev. E **54**, 993 (1996).
[17] A. Tamura and T. Ichinokawa, Surf. Sci. **136**, 437 (1984).
[18] S. Ljunggren and J. C. Eriksson, J. Chem. Soc. Faraday Trans. **2**, 1553 (1989).
[19] M. Zulauf and H.-F. Eicke, J. Phys. Chem. **83**, 480 (1979).
[20] C. Dunn, B. H. Robinson, and F. J. Leng, Spectrochim. Acta, Part A **46**, 1017 (1990).
[21] A. Maitra, J. Phys. Chem. **88**, 5122 (1984).
[22] M. D'Angelo, G. Onori, and A. Santucci, Nuovo Cimento Soc. Ital. Fis. **16**, 1601 (1994).
[23] C. A. Martin and L. J. Magid, J. Phys. Chem. **85**, 3938 (1981).
[24] J. T. Kindt and C. A. Schmuttenmaer, J. Phys. Chem. **100**, 10 373 (1996).
[25] C. Rønne *et al.,* J. Chem. Phys. **107**, 5319 (1997).
[26] D. M. Mittleman, M. C. Nuss, and V. L. Colvin, Chem. Phys. Lett. **275**, 332 (1997).
[27] T. Hanai, T. Imakita, and N. Koizumi, Colloid Polym. Sci. **260**, 1029 (1982).
[28] The parameter F depends on the thickness of the AOT shell, which has been independently determined by NMR measurements [21]. Since all other quantities in Eqs. (1) and (2) are known, this deconvolution procedure contains no adjustable parameters.
[29] M. Kotlarchyk, J. S. Huang, and S.-H. Chen, J. Phys. Chem. **89**, 4382 (1985).
[30] J. Ricka, M. Borkovec, and U. Hofmeier, J. Chem. Phys. **94**, 8503 (1991).
[31] J. Faeder and B. M. Ladanyi, J. Phys. Chem. B **104**, 1033 (2000).
[32] D. G. Peck, R. S. Schechter, and K. P. Johnston, J. Phys. Chem. **95**, 9541 (1991).
[33] A. Amararene *et al.,* Phys. Rev. E **61**, 682 (2000).
[34] E. Duval, Phys. Rev. B **46**, 5795 (1992).